B. Dose calculations in a thorax phantom and in human lung

Dosimetry properties of the kilovoltage 3DCSRT system were investigated to irradiate targets in a thorax phantom and human lung. The thorax phantom consisted of three types of densities: the density of the lung region was 0.3 g/cc, the densities of the tumor (2 cm ϕ sphere situated at the center of the right lung) and other soft-tissue equivalent material were 1.0 g/cc. The density of the spine was 1.3 g/cc. CT measurements of the thorax phantom were performed to obtain CT images. Patient-specific CT images of lung tumors ($\approx$2 cm ϕ) were used to assess dose distributions in real situations. In both cases (e.g., thorax phantom and human lung), the thickness of CT slices was 2 mm and the matrix size of each slice was 512 pixels$\times$512 pixels for a dimension of 50 cm along the x and y axes.

To calculate dose distributions with Monte Carlo, CT values of images need to be converted into physical densities called egs4phant.[22,23] All CT numbers in CT images in this study were converted to egs4phant data using their corresponding electron-density data. The matrix size of egs4phant data was reduced to 256 pixels$\times$256 pixels; these data were used in the Monte Carlo dose calculation system. Voxel size of the data in egs4phant was 0.195$\times$0.195$\times$0.2 cm.

Three non-coplanar converging arcs around the center of the gross tumor volume (GTV) were employed to calculate Monte Carlo dose with the thorax phantom and human lung for 147.5, 200, 300, and 500 kVp x-ray energy. For each of three different couch angles, 0° and ±25°, the gantry rotation around the target was 200° both for the thorax phantom (160° to 360°) and the human lung (190° to 30°). A 3 cm $\times$3 cm beam size was used to investigate the dose distribution by using the phase space file for the corresponding energy as previously calculated. All dosimetry calculations were performed using DOSXYZnrc code, which has nine different options for defining a beam source. In our calculations we used source 8, which allowed us to use phase space sources from multiple directions to produce non-coplanar arcs.

To compare dose distributions of kVp energy for the kilovoltage 3DCSRT system with MV energies of a linac system, Monte Carlo dose calculations were performed with the same CT data and arc information for 4, 6, and 10 MV energy.[24] Beam source 7 was used to produce non-coplanar arcs from multiple directions using energy spectra. In all cases, 300$\times 10^6$ photon events were used, and dose errors were within 1.0%. The phase space data was redistributed and recycled when used as beam source.

Recently, we have developed an interface to analyze DOSXYZnrc dose data on a commercial RTP system (XiO version 4.2, CMS, St. Louis, USA). With this interface, the DOSXYZnrc Monte Carlo dose-file format can be converted to XiO RTP dose-file format and the dose file of the XiO RTP can be replaced with the Monte Carlo dose-file. The necessary information required in conversion procedures are patient ID, planning ID, and coordinates of the center of the coronal image on the XiO RTP system. This system leads us to analyze the Monte Carlo dose on a XiO RTP system in the form of either integral or differential DVH and analysis of dose homogeneity in terms of maximum, minimum, and average dose described in International Commission on Radiation Units and Measurements (ICRU) reports 50 and 60.[25,26]

To analyze our Monte Carlo dose on a XiO RTP system, all thorax phantom and human CT images were transferred to the XiO RTP system and an arbitrary RTP plan with arbitrary energy was generated to analyze DVH of Monte Carlo dose on a defined structure like GTV and planning target volume (PTV). A 5 mm margin with GTV was used to define PTV. Using our interface, all Monte Carlo doses were analyzed with the XiO RTP system.

C. Dose calculation and measurements in water phantom

The simulated system was verified by comparing measured and calculated percentage of depth dose (PDD) values and profiles in water phantom for the x-ray energy of 120 and 147.5 kVp. A water phantom with dimensions of 20 cm$\times$20 cm$\times$20 cm was used to investigate PDD and profiles with DOSXYZnrc Monte Carlo simulations.[22,23] The beam size at an SSD of 50 cm was 2 cm$\times$2 cm. In all cases, full phase-space source file was considered. To confirm accuracy of the PDD results, a CT x-ray beam operated at 120 and 147.5 kVp with 400 mA was used to irradiate a solid water phantom (WE-211, Kyoto Kagaku Co., Kyoto, Japan) with normal incidence. The tissue maximum ratio (TMR) was measured with a pinpoint ionization chamber (IC) (PTW-31006) to calculate PDD. In TMR measurement, the absolute charge rate (C/min) at each phantom depth was measured with the IC chamber and converted to absolute dose rate. Beforehand, the experimental IC was calibrated against a standard IC (PTW TN30001, PTW-Freiburg, Freiburg, Germany). The center of the active volume of the IC was adjusted to the center of the beam with laser markers, and fine adjustment was performed with real-time two-dimensional scout view x-ray image from the CT interface.

The PDD was also measured with GAFCHROMIC® XR film type R (International Specialty Products-ISP, Wayne, NJ, USA) in a water phantom with dimensions of 20 cm $\times$20 cm$\times$20 cm for normal incidence of the beam. Film (originally 14 in.$\times$17 in.) was cut to 10 cm$\times$20 cm and clamped to place its height along the beam direction for an exposure of 2 min. The film was scanned with a color scanner (ES-2000, Seiko Epson Corporation, Nagano, Japan) and saved as an image; pixel values from each region of interest on the scanned image were converted to dose after background subtraction with proper calibration.[27] All measured PDD values were compared with simulated PDD values.

Beam profiles along the center of the x (in-line) and y (cross-line) directions at a phantom depth of 5 and 10 cm were measured with GAFCHROMIC film for a distance of −2.5 cm to +2.5 cm with an interval of 1 mm.

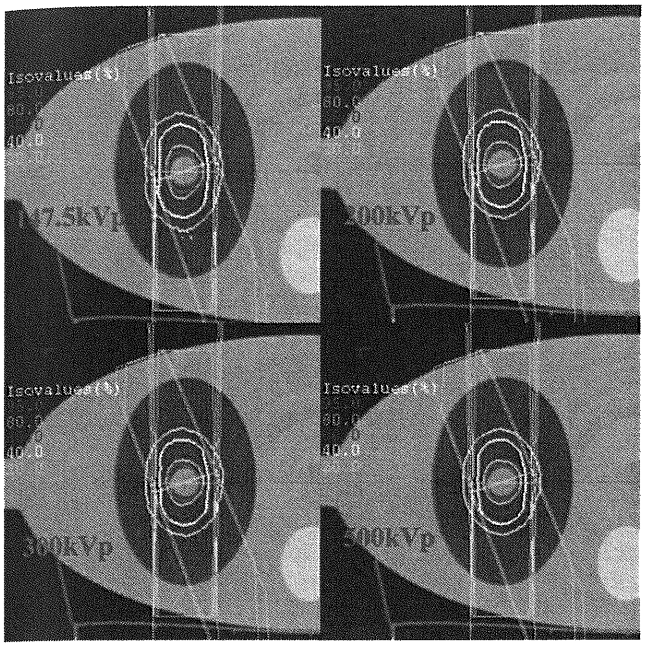

FIG. 2. Monte Carlo dose data calculated in a thorax phantom for x-ray energy of 147.5, 200, 300, and 500 kVp are displayed on the XiO RTP system. Dose distributions on isocenter slice are shown in the figure. In all cases, doses were normalized with the dose at the center of the gross tumor volume (GTV). For three couch angles, 0° and ±25° the gantry rotations were 200° (clockwise direction 160° to 360°).

III. RESULTS

A. Dose calculations in a thorax phantom and human lung

Monte Carlo dose distributions to tumor in a thorax phantom and in human lung with DOSXYZnrc for the x-ray energy of 147.5, 200, 300, and 500 kVp and MV energy of 4, 6, and 10 MV were calculated using non-coplanar multiple arcs with a common isocenter. All Monte Carlo doses were analyzed with the XiO RTP system using the interface we developed. Isodose curves appearing on the XiO RTP system for the x-ray energy of 147.5, 200, 300, and 500 kVp are shown in Fig. 2. All these curves were normalized with the dose at the center of GTV.

Comparative studies of integral and differential DVH values of GTV and PTV for kVp and MV energies are shown in Figs. 3 and 4, respectively. In Fig. 3, the integral DVHs of kVp energy were better than the DVHs of MV energy, but within all histograms, the 500 kVp data were better than the data for all other energies.

In the differential DVH data of GTV for all kVp, energies ranged from almost 80% to 100% and the dose peak for 300 and 500 kVp was around 92% dose; however, the 200 kVp dose peak was shifted at 87% dose. For 4 MV energy range, the dose distribution was similar to kVp energy and the dose peak was at 97%. The dose peaks of 6 and 10 MV energy were flat compared with other energies, and a trend of dose distributions toward the lower dose can be seen with increases in energy. When a 0.5 cm margin was added to GTV to define PTV, both the integral and differential DVHs of PTV for all MV energies were worse than DVHs of GTV (Fig. 4) and the tendency to dose distributions below 80% increased. Notably, the integral and differential DVHs of PTV for kVp energies were still better than histograms for MV energies.

The minimum, maximum, and average doses within the GTV of the thorax phantom for the energies considered in these studies are shown in Table I. Dose homogeneity only within the GTV was defined as the quotient of minimum and average dose. In Table I, although the minimum and average doses of the kVp energies increased with increasing energy, in contrast those doses decreased with increasing MV energy. But in all cases the dose homogeneity of kVp energies was better than the MV energies.

The dose distribution for each energy was reconstructed on transverse, coronal and sagittal planes taken through the isocenter, and compared with the distribution for 4 MV (see Fig. 5). The comparisons of dose distributions in the form of a dose map were generated from the dose output file of

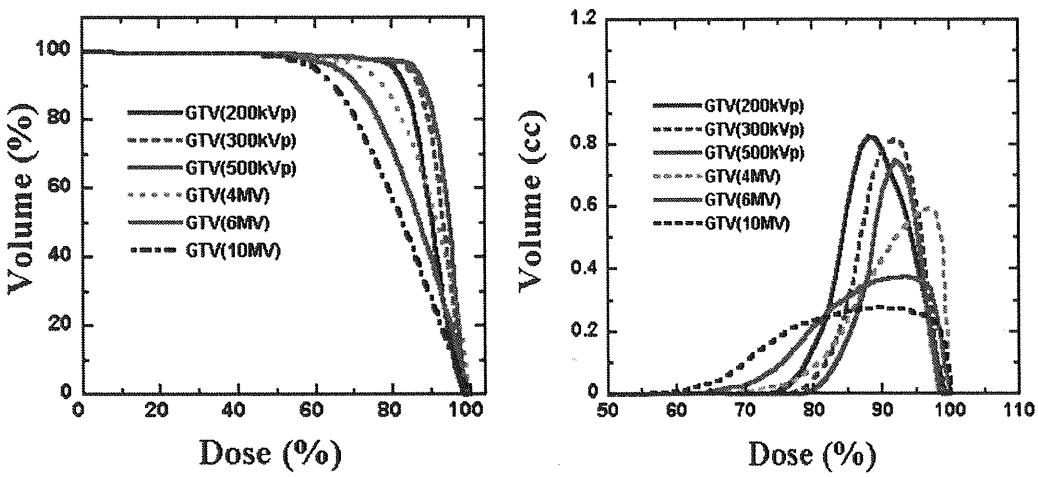

FIG. 3. Integral (left) and differential (right) dose volume histograms (DVHs) of gross tumor volume (GTV) in a thorax phantom for Monte Carlo doses of kVp and MV energies. All data were analyzed with the radiotherapy planning system. Size of GTV was 2 cm diameter; beam size was 3 cm×3 cm.

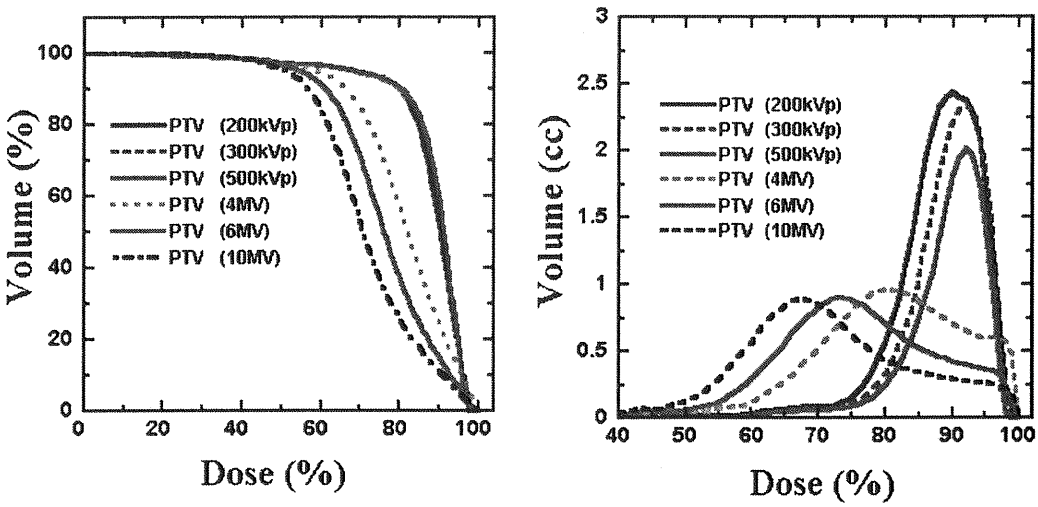

FIG. 4. Integral (left) and differential (right) dose volume histograms (DVHs) of planning target volume (PTV) in a thorax phantom for Monte Carlo doses of kVp and MV energies. A 0.5 cm margin with the GTV defined PTV. Size of PTV was 3 cm diameter; beam size was 3 cm×3 cm.

DOSXYZnrc. The dose maps for first, isocenter, and last slices of GTV are shown in Fig. 6. The absorption of dose to bone from kVp x rays is demonstrated by the calculations, and easily seen in Figs. 5 and 6. It can be clearly seen that a relatively high dose appears at the rib bones when the target in the human lung is irradiated with low-energy x ray. The range of apparent dose to the ribs was 80%–90% for 200 kVp, 40%–60% for 300 kVp and 20%–40% for 500 kVp. Rib doses were higher for low-energy x rays: With increasing x-ray energy, dose to the bones decreased. The DVHs of GTV delineated on the human lung tumor for 200, 300, and 500 kVp with 4 MV energy are shown in Fig. 7. The DVH of 500 kVp is better than the histograms of other energies. To analyze DVHs on the XiO RTP system, the doses in all cases were normalized with dose of center of GTV.

B. Dose calculations and measurements in water phantom

Comparison of experimental and simulated PDD values only for 120 kVp energy is shown in Fig. 8 using a logarithmic scale. TMR measurements with IC were performed up to a depth of 12 cm, and those data were converted to PDD. The simulated PDD and actual PDD values obtained from TMR measurements with IC matched up well with each other. In film measurements, the PDD obtained up to 9 cm of depth matched up well with the PDD obtained from simulation and IC measurement; however, at depths greater than 9 cm those values were relatively high.

The measured and simulated profiles match up well with each other and those profiles for x-ray energy of 120 kVp at a depth 10 cm in a water phantom are shown in Fig. 9. All data were normalized with their corresponding maximum values.

TABLE I. Dose homogeneity of the kVp and MV energies in the GTV of the thorax phantom. In all cases, maximum dose was normalized to 100%.

Energy	Minimum dose (%)	Average dose (%)	Dose homogeneity (minimum dose/mean dose)
147 kVp	80.4	90.2±6.6	0.89
200 kVp	83.3	92.1±5.1	0.90
300 kVp	84.2	92.7±5.3	0.91
500 kVp	88.9	94.0±4.2	0.95
4 MV	70.8	85.4±9.1	0.83
6 MV	65.2	82.6±9.4	0.79
10 MV	60.5	80.3±9.2	0.75

IV. DISCUSSION

BEAMnrc Monte Carlo[21] based on EGS4[28] is a well-recognized code to provide the calculation of particle transport through the accelerator head, and DOSXYZnrc[22] is a general-purpose Monte Carlo EGSnrc[29] user code for three-dimensional absorbed dose calculations. The DOSXYZnrc code allows sources such as a monoenergetic diverging or parallel beam, phase-space data generated by a BEAMnrc simulation or a model-based beam reconstruction produced by BEAMDP.[23] Different types of source to model the beam from energy spectra including phase-space files can be used in DOSXYZnrc. Sources 7 and 8 have options to define multiple beam directions using an energy spectra and phase-space source, respectively. The user may define the incident angles of the phase-space beam by changing angles theta and phi.[22] In the polar coordinate system, the polar angle, theta, has a range of 0°–180°, and the azimuthal angle phi has a range of 0°–360°. In our simulations, non-coplanar arcs were defined by changing the angles theta and phi. Although the phase-space file is inconvenient to handle due to its large size, it nevertheless gives accurate dose results,[22] and this was the method used in this study. Although 300 m$\times 10^6$ electron events were used to simulate the x-ray tube, the total number of photons observed in the phase space files were 12 m$\times 10^6$ to 18 m$\times 10^6$, depending on the energy and collimator size. To reduce statistical uncertainty, 300 million

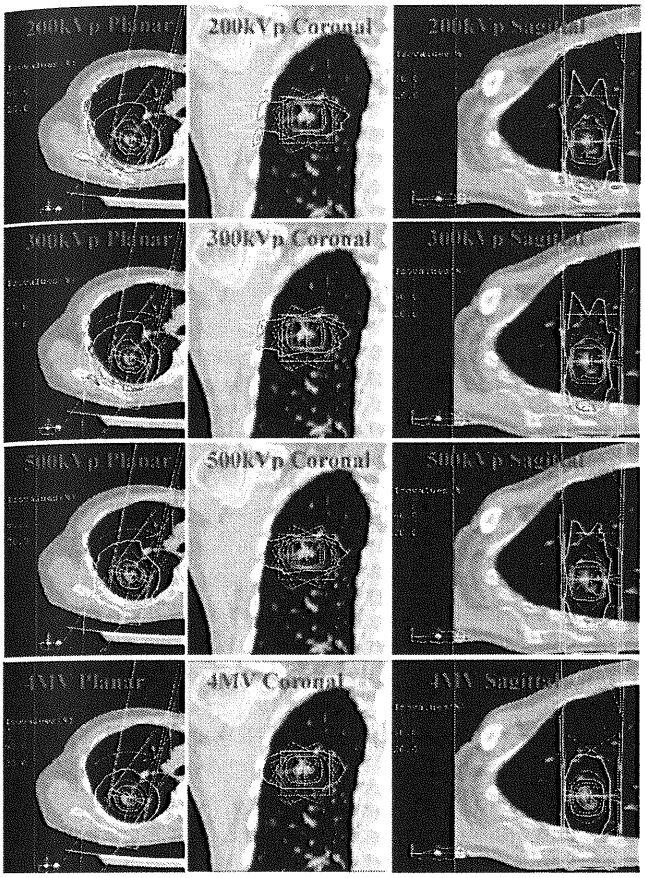

FIG. 5. Monte Carlo dose calculated in a human lung tumor for x-ray energies of 200, 300, and 500 kVp, as well as 4 MV. Dose distributions on the planar (isocenter slice), coronal, and sagittal images displayed with XiO RTP system are shown in the figure with beam arrangement. In all cases, doses were normalized with the isocenter dose within the gross tumor volume (GTV). Beam directions of three non-coplanar arcs for gantry rotations 200° (clockwise direction 190° to 30°) and couch angle 0° and ±25° appeared on the coronal image.

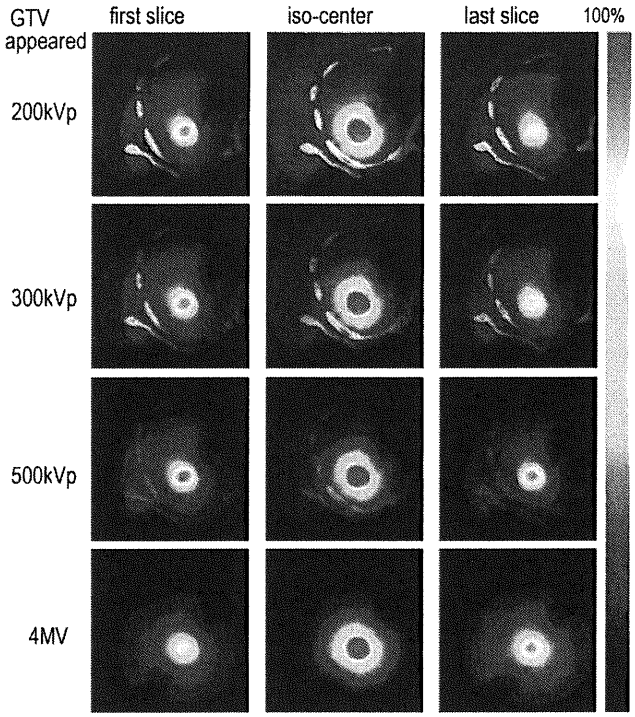

FIG. 6. Monte Carlo dose map in a human lung tumor irradiated with kVp and MV energy. Dose distributions appearing in the GTV of the first, isocenter, and last slices are shown in the figure.

photon events were used in the dose calculation procedures, and the phase-space data were redistributed and recycled.[30] In its present form, our CT system's highest operating voltage is 147.5 kVp. Therefore, for a kilovoltage 3DCSRT system with 200, 300, and 500 kVp, 147.5 kVp energy was also investigated in the simulation study.

Phantom dosimetry to validate the system was performed with 120 and 147.5 kVp x-ray energy. The pinpoint IC with a volume 0.015 cm^3 is designed for stereotactic field measurements in radiation therapy, but because we are investigating a narrow beam 2 cm × 2 cm field, we used this chamber for our experiments. As the active volume of the IC is very small, the center of that volume was positioned at the center of the x-ray beam with laser beams and a two-dimensional scout view x-ray imaging from the CT interface. The TMR method was used in this study to obtain PDD data with pinpoint chamber measurement. Usually TMR can be measured "manually" by lowering the detector in the phantom and raising the water phantom with the same distance, or it can be derived from the PDD results.[31] In our study we used a solid water phantom and pinpoint chamber. Because it is very important to place the active small volume of the chamber at the center of the x-ray beam, the positioning of the chamber to measure PDD for each depth of the water phantom is time consuming; small displacements of the chamber may lead to error in the absolute measurements. Therefore, TMR measurements were performed in this study and necessary correction factors[32] were used to convert the TMR results into PDD results. The pinpoint chamber used in the study was cross-calibrated against a secondary standard ionization chamber and electrometer system calibrated by the Japan Calibration Service System (JCSS) calibration laboratory.

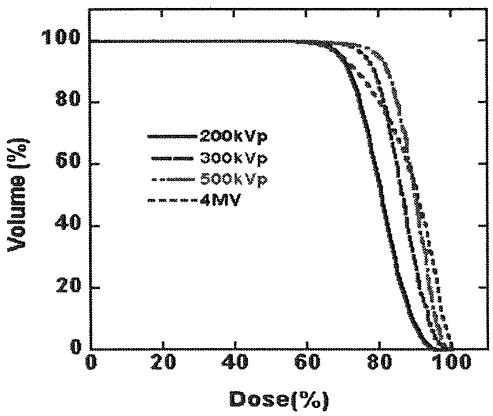

FIG. 7. Dose volume histograms (DVHs) of GTV in a human lung for Monte Carlo doses of kVp and MV energies. Size of the GTV was 1.7 cm diameter; beam size was 3 cm × 3 cm.

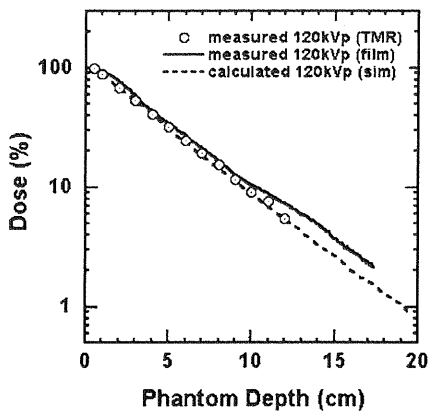

FIG. 8. Comparison of simulated and experimental percentage of depth dose (PDD) values for 120 kVp. Ionization chamber and film were used in experiments to calculate PDD. An ionization chamber was used to measure PDD in a water equivalent material with a depth of 12 cm. Both in the film measurement and simulation water phantom, a depth of 20 cm was considered.

It has been reported that GAFCHROMIC® XR film type R is suitable for dosimetry of the lower-energy x-rays used in diagnostic x-ray, computer tomography, and superficial/orthovoltage therapy.[33] We used this film to measure PDD data in our experiment (Fig. 8). Dosimetry with GAFCHROMIC film after exposure can be obtained from density data derived with a densitometer[33] or pixel values of images after scanning the film with a scanner.[27] In our study we used a scanner to measure pixel values, and those pixel values were converted to dose according to the calibration procedures described elsewhere.[27,33]

The PDD results of the film up to 9 cm were a good match with PDD data obtained from IC measurement and Monte Carlo simulation. However, at depths greater than 9 cm the PDD values from film measurements were higher than those obtained with IC and Monte Carlo simulations. It has been shown that GAFCHROMIC XR film type R has strong energy dependency and the sensitivity of the film around an effective energy of 40 keV is higher than sensitivity at other energies.[33] Over 300 keV, film sensitivity is almost constant with effective energy. In our PDD measurement with the film, we found that by increasing the depth of the phantom beam, intensity became weaker and low-energy scattered photons gradually increased. Those low-energy scattered photons may lead to higher film sensitivity as well as higher doses.

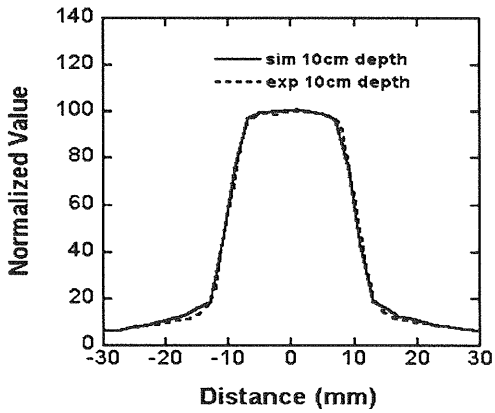

FIG. 9. Experimental and simulated beam profiles at 10 cm depth in a water equivalent phantom with a source-center distance of 60 cm. The solid and dashed lines represent simulated and experimental profiles, respectively.

For kilovoltage 3DCSRT with the thorax phantom, the integral DVHs of kVp energies (Figs. 3 and 4) were better than the histograms for MV energies. The reason for these improvements in DVHs for kVp energies was clarified from the corresponding differential DVHs (Figs. 3 and 4). As photon energy increases, distributions of lateral scatter electrons are increased, and thus there are wide ranges of lower doses (40%–100%) within the target for MV energies. When a 0.5 cm margin is added to the target, the effect of a lower dose within the PTV becomes more prominent, even for 4 MV energy (Fig. 4). In a previous study it has been mentioned that the non-coplanar technique with the lower energy photons covered the tumor with the greatest isodose at the tumor periphery without tangential sparing in the coronal plane,[34] and this we found consistent with our results.

It is important to note that in order to visualize MC doses on the XiO RTP system, an arbitrary plan was first generated using standard beams on the XiO RTP system. The XiO dose data was then substituted with the MC dose file in that arbitrary plan. Therefore, the field edges depicted in Figs. 2 and 5 are from arbitrary generated plan and do not correctly represent the field dimensions.

To investigate dose homogeneity (Table I) we considered only GTV; wide range of lower doses in PTV will increase the dose inhomogeneity. In the thorax phantom, there were no highly dense media such as bone along the path of the beam before incidence on the target; uniform dose distribution appeared around the target for all kVp energy (Fig. 2). In the case of human CT data (Figs. 5 and 6), the incident beam attenuated more at rib bones due to high density and caused an elevation in absorbed dose due to photoelectrons because low-energy x rays are sensitive to high-Z value materials. However, for 200 kVp x-ray energy, the range of the rib dose was 80%–90%. With increases in energy up to 500 kVp, the range of the rib dose was reduced to the 20%–40% mark.

If we consider activity in terms of dose homogeneity only, a medium-energy x ray such as 200 kVp can provide almost homogeneous dose distribution for a kVp 3DCSRT system. However, if we consider both dose homogeneity and dose absorption at the ribs, a minimum of 500 kVp is suitable for the lung kVp 3DCSRT system.

ACKNOWLEDGMENTS

This research is part of the projects (IMAGINE) supported by the Japan Science and Technology Agency (JST), CREST program.

[a]Present address: Department of Medical Physics and Bioengineering, Christchurch Hospital, Christchurch, New Zealand.
[b]Author to whom correspondence should be addressed. Electronic mail: kunieda-mi@umin.ac.jp

[1]J. D. Graham, A. P. Warrington, S. S. Gill, and M. Brada, "A noninvasive, relocatable stereotactic frame for fractionated radiotherapy and multiple

imaging,"Radiother. Oncol. **21**, 60–62 (1991).
[2]G. H. Hartmann, B. Bauer-Kirpes, C. F. Serago, and W. J. Lorenz, "Precision and accuracy of stereotactic convergent beam irradiations from a linear accelerator," Int. J. Radiat. Oncol., Biol., Phys. **28**, 481–492 (1994).
[3]H. M. Kooy, S. F. Dunbar, N. J. Tarbell, E. Mannarino, N. Ferarro, S. Shusterman, M. Bellerive, L. Finn, C. V. McDonough, and J. S. Loeffler, "Adaptation and verification of the relocatable Gill-Thomas-Cosman frame in stereotactic radiotherapy," Int. J. Radiat. Oncol., Biol., Phys. **30**, 685–691 (1994).
[4]A. P. Warrington, R. W. Laing, and M. Brada, "Quality assurance in fractionated stereotactic radiotherapy," Radiother. Oncol. **30**, 239–246 (1994).
[5]D. Yeung, J. Palta, J. Fontanesi, and L. Kun, "Systematic analysis of errors in target localization and treatment delivery in stereotactic radiosurgery (SRS)," Int. J. Radiat. Oncol., Biol., Phys. **28**, 493–498 (1994).
[6]H. Blomgren, I. Lax, I. Naslund, and R. Svanstrom, "Stereotactic high-dose fraction radiation therapy of extracranial tumors using an accelerator. Clinical experience of the first thirty-one patients," Acta Oncol. (Madr) **34**, 861–870 (1995).
[7]Y. C. Lo, C. C. Ling, and D. A. Larson, "The effect of setup uncertainties on the radiobiological advantage of fractionation in stereotactic radiotherapy," Int. J. Radiat. Oncol., Biol., Phys. **36**, 1113–1119 (1996).
[8]M. Riboldi, G. Baroni, M. F. Spadea, F. Bassanini, B. Tagaste, C. Garibaldi, R. Orecchia, and A. Pedotti, "Robust frameless stereotactic localization in extra-cranial radiotherapy," Med. Phys. **33**, 1141–1152 (2006).
[9]M. A. Ebert, S. F. Zavgorodni, L. A. Kendrick, S. Weston, and C. S. Harper, "Multi-isocenter stereotactic radiotherapy: implications for target dose distributions of systematic and random localization errors," Int. J. Radiat. Oncol., Biol., Phys. **51**, 545–554 (2001).
[10]E. Yorke, L. Harisiadis, B. Wessels, H. Aghdam, and R. Altemus, "Dosimetric considerations in radiation therapy of coin lesion of the lung," Int. J. Radiat. Oncol., Biol., Phys. **34**, 481–487 (1996).
[11]M. A. Hunt, G. E. Desobry, B. Fowble, and L. R. Coia, "Effect of low-density lateral interfaces on soft-tissue doses," Int. J. Radiat. Oncol., Biol., Phys. **37**, 475–482 (1997).
[12]K. E. Ekstrand and W. H. Barnes, "Pitfalls in the use of high energy x-rays to treat tumor in the lung," Int. J. Radiat. Oncol., Biol., Phys. **18**, 249–252 (1990).
[13]B. A. Fraass, A. S. Lichter, D. L. McShan, B. R. Yanke, R. F. Diaz, K. S. Yeakel, and J. van de Geijn, "The influence of lung density corrections on treatment planning for primary breast cancer," Int. J. Radiat. Oncol., Biol., Phys. **14**, 179–190 (1988).
[14]T. R. Mackie, E. el-Khatib, J. Battista, J. Scrimger, J. Van Dyk, and J. R. Cunningham, "Lung dose corrections for 6- and 15-MV x rays," Med. Phys. **12**, 327–332 (1985).
[15]M. E. Young and R. O. Kornelsen, "Dose corrections for low-density tissue inhomogeneities and air channels for 10-MV x rays," Med. Phys. **10**, 450–455 (1983).
[16]H. Saitoh, T. Fujisaki, R. Sakai, and E. Kunieda, "Dose distribution of narrow beam irradiation for small lung tumor," Int. J. Radiat. Oncol., Biol., Phys. **53**, 1380–1387 (2002).
[17]K. S. Iwamoto, A. Norman, A. R. Kagan, M. Wollin, A. Olch, J. Bellotti, M. Ingram, and R. G. Skillen, "The CT scanner as a therapy machine," Radiother. Oncol. **19**, 337–343 (1990).
[18]K. S. Iwamoto, A. Norman, D. B. Freshwater, M. Ingram, and R. G. Skillen, "Diagnosis and treatment of spontaneous canine brain tumors with a CT scanner," Radiother. Oncol. **26**, 76–78 (1993).
[19]J. H. Rose, A. Norman, M. Ingram, C. Aoki, T. Solberg, and A. Mesa, "First radiotherapy of human metastatic brain tumors delivered by a computerized tomography scanner (CTRx)," Int. J. Radiat. Oncol., Biol., Phys. **45**, 1127–1132 (1999).
[20]H. M. Deloar, E. Kunieda, T. Kawase, H. Saitoh, M. Ozaki, T. Fujisaki, A. Myojoyama, K. Saito, S. Takagi, O. Sato, and A. Kubo, "Monte Carlo Simulations for Stereotactic Radiotherapy System with Various Kilovoltage X-ray Energy," Third international EGS Workshop, High Energy Physics Center, Japan, Aug, 2004, *KEK Proc*, pp. 172–179.
[21]D. W. O. Rogers, B. A. Faddegon, G. X. Ding, C. M. Ma, J. Wei, and T. R. Mackie, "BEAM: A Monte Carlo code to simulate radiotherapy treatment units," Med. Phys. **22**, 503–524 (1995).
[22]B. R. B. Walters and D. W. O. Rogers, "DOSXYZnrc Users Manual, NRCC Report PIRS-794 (Ottawa: NRCC)," 2002.
[23]J. A. Treurniet, B. R. B. Walters, and D. W. O. Rogers, "BEAMnrc, DOSXYZnrc and BEAMDP GUI User's Manual," NRC Report PIRS 0623(rev C).
[24]R. Mohan, C. Chui, and L. Lidofsky, "Energy and angular distributions of photons from medical linear accelerators," Med. Phys. **12**, 592–597 (1985).
[25]ICRU Report 50, "Prescribing, recording and reporting photon beam therapy," International Commission on Radiation Units and Measurements, Bethedesa, MD, 1992.
[26]ICRU Report 62 (Suppl. to ICRU Report 50), "Prescribing, Recording and Reporting Photon Beam Therapy," International Commission on Radiation Units and Measurements, Bethedesa, MD, 1999.
[27]M. Yamauchi, T. Tominaga, O. Nakamura, R. Ueda, and M. Hoshi, "GAFChromic film dosimetry with a flatbed color scanner for Leksell Gamma Knife therapy," Med. Phys. **31**, 1243–1248 (2004).
[28]W. R. Nelson, H. Hirayama, and D. W. O. Rogers, "The EGS4 Code System," Report SLAC-265, Stanford Linear Accelerator Center, Stanford, California, 1985.
[29]I. Kawrakow and D. W. O. Rogers, "The EGSnrc Code System: Monte Carlo simulation of electron and photon transport," Technical Report PIRS-701, National Research Council of Canada, Ottawa, Canada, 2000.
[30]B. R. B. Walters, I. Kawrakow, and D. W. O. Rogers, "History by history statistical estimators in the BEAM code system," Med. Phys. **29**, 2745–2752 (2002).
[31]L. J. Battum, M. Essers, and P. R. Storchi, "Conversion of measured percentage depth dose to tissue maximum ratio values in stereotactic radiotherapy," Phys. Med. Biol. **47**, 3289–3300 (2002).
[32]F. M. Khan, *The Physics of Radiation Therapy* (Williams & Wilkins, Baltimore, 1984).
[33]S. A. Dini, R. A. Koona, J. R. Ashburn, and A. S. Meigoonia, "Dosimetric evaluation of GAFCHROMIC XR type T and XR type R films," J. Appl. Clin. Med. Phys. **6**, 114–134 (2005).
[34]P. M. DesRosiers, V. P. Moskvin, C. M. DesRosiers, R. D. Timmerman, M. E. Randall, and L. S. Papiez, "Lung cancer radiation therapy: Monte Carlo investigation of "under dose" by high energy photons," Technol. Cancer Res. Treat. **3**, 289–294 (2004).

ELSEVIER

Int. J. Radiation Oncology Biol. Phys., Vol. 65, No. 1, pp. 107–111, 2006
Copyright © 2006 Elsevier Inc.
Printed in the USA. All rights reserved
0360-3016/06/$–see front matter

doi:10.1016/j.ijrobp.2005.10.031

CLINICAL INVESTIGATION **Lung**

HIGH-DOSE PROTON BEAM THERAPY FOR STAGE I NON–SMALL-CELL LUNG CANCER

KEIJI NIHEI, M.D., TAKASHI OGINO, M.D., SATOSHI ISHIKURA, M.D., AND HIDEKI NISHIMURA, M.D.

Radiation Oncology Division, National Cancer Center Hospital East, Kashiwa, Chiba, Japan

Purpose: To evaluate retrospectively the safety and efficacy of high-dose proton beam therapy (PBT) for Stage I non–small-cell lung cancer (NSCLC).

Methods and Materials: Between 1999 and 2003, 37 patients were treated in our institution. The indications for PBT were pathologically proven NSCLC, clinical Stage I, tumor size ≤5 cm, medically inoperable or refusal of surgery, and written informed consent. A total dose of 70–94 Gy_E was delivered in 20 fractions (3.5–4.9 Gy_E per fraction).

Results: Patient characteristics (number of patients) were as follows: Stage IA/IB, 17 of 20; medically inoperable/refusal of surgery, 23/14; total dose 70/80/88/94 Gy_E, 3/17/16/1. With a median follow-up period of 24 months, the 2-year local progression-free and overall survival rates were 80% and 84%, respectively. The 2-year locoregional relapse-free survival rates in Stage IA and Stage IB were 79% and 60%, respectively. No serious acute toxicity was observed. Late Grades 2 and 3 pulmonary toxicities were observed in 3 patients each. Of these 6 patients, 5 had Stage IB disease.

Conclusions: Proton beam therapy is a promising treatment modality for Stage I NSCLC, though locoregional relapse and late pulmonary toxicities in Stage IB patients were substantial. Further investigation of PBT for Stage I NSCLC is warranted. © 2006 Elsevier Inc.

Proton beam therapy, Radiotherapy, High dose, Non–small-cell lung cancer, Stage I.

INTRODUCTION

Lung cancer continues to be the leading cause of cancer death worldwide. Surgical resection for Stage I (T1–2N0) non–small-cell lung cancer (NSCLC) results in 5-year overall survival rates of approximately 60–70% and remains the standard treatment for this population (1, 2).

Some patients with Stage I NSCLC cannot undergo surgery, owing to preexisting comorbidities, advanced age, or refusal. Conventional radiotherapy alone has been used as the next alternative approach for these patients with early-stage NSCLC, but outcomes have been inferior to those of surgical resection (3–6), although there is a potential selection bias due to stage migration and patients' general conditions. Some studies reported a benefit of dose escalation, suggesting that higher doses of radiation therapy might improve both local tumor control and survival (7). However, conventional radiotherapy often cannot deliver higher doses to the tumor without increasing adverse effects.

Proton beams have a distinct physical advantage over conventional photon beams. Proton beams have a low entrance dose, a maximal dose at any prescribed depth, called the "Bragg peak," and no exit dose. The "Bragg peak" can be spread out and shaped to conform to the depth and volume of an irregular target. Proton beam therapy (PBT) can thus create an inherently three-dimensional conformal dose distribution without extra dose to the surrounding normal tissue compared with conformal photon treatment.

At the National Cancer Center Hospital East, we introduced PBT for clinical use in 1998. In the present study, we retrospectively evaluated the safety and efficacy of high-dose PBT for Stage I NSCLC.

METHODS AND MATERIALS

We started a Phase I dose escalation study of PBT for Stage I NSCLC in December 1999 for the purpose of determining the maximum tolerated dose. The eligibility criteria were (*1*) pathologically proven NSCLC, (*2*) clinical Stage I, (*3*) tumor size ≤5 cm in diameter, (*4*) pO_2 ≥60 torr, (*5*) medically inoperable or refusal of surgery, (*6*) Zubrod performance status 0–2, and (*7*) written informed consent. Patients received escalating doses of PBT in 20 fractions (fx) over 4 or 5 weeks as follows: level 1: 70 Gy_E (3.5 Gy_E/fx); level 2: 80 Gy_E (4.0 Gy_E/fx); level 3: 88 Gy_E (4.4 Gy_E/fx); level 4: 94 Gy_E (4.7 Gy_E/fx); level 5: 98 Gy_E (4.9 Gy_E/fx). Dose-limiting toxicity included Grade 4 radiation dermatitis and other Grade 3 nonhematologic toxicities.

Reprint requests to: Keiji Nihei, M.D., National Cancer Center Hospital East, Radiation Oncology Division, 6-5-1, Kashiwanoha, Kashiwa, Chiba, Japan. Tel: (+81) 4-7133-1111; Fax: (+81) 4-7131-4724; E-mail: knihei@east.ncc.go.jp

Presented at the 41st Annual Meeting of the American Society of Clinical Oncology, Orlando, Florida, May 13–17, 2005.

Received Aug 12, 2005, and in revised form Oct 7, 2005. Accepted for publication Oct 18, 2005.

In total, 10 patients were enrolled in the dose escalation study. Three patients were enrolled in each of levels 1 to 3. The first patient enrolled in level 4 (94 Gy_E) suffered symptomatic radiation pneumonitis after PBT, which resulted in early closure of the study. In July 2001, PBT in Japan was authorized by the government as a highly advanced medical technology, and thereafter an additional 27 patients who had met the criteria above were treated by PBT on an off-study basis. Thirteen of them received a total dose of 88 Gy_E (4.4 Gy_E/fx), and the other 14 patients with poorer pulmonary function received a total dose of 80 Gy_E (4.0 Gy_E/fx) at the discretion of the radiation oncologists.

For PBT planning, thoracic CT images were obtained in the exhalation phase with a respiratory gating system. Patients were immobilized in the supine position on a body cast with both arms above the head. The primary tumor was delineated on a lung window as the gross tumor volume. The clinical target volume was defined as the gross tumor volume with a margin of 8 mm in all directions for subclinical tumor extension. The planning target volume was defined as the clinical target volume with a setup margin of 5 mm and with an internal margin of 5 mm for uncertainty of respiratory motion. Two or four portals of proton beams were arranged in the optimal angles to avoid excessive dose exposure to the normal lung and skin. Range modulation by bar-ridge filters was used to generate Spread-Out Bragg Peak, and 150-MeV or 190-MeV proton beams were selected to conform to the target volume. Daily verification of patient positioning was performed by the image subtraction method with digital radiography (8). Respiratory gating was used in all patients during the treatment to deliver proton beams to the target volume in the exhalation phase. The relative biologic effectiveness of our proton beam was 1.1 (Gy_E = proton Gy × 1.1), according to a previous animal examination (9).

After PBT, patients were examined every 3 months for the first 2 years and every 6 months thereafter. Chest X-ray films and CT images were also obtained at the same time to evaluate the local tumor response and other radiographic findings.

Tumor response was evaluated according to the previously published Response Evaluation Criteria in Solid Tumors (10). A complete response indicated that the tumor had completely disappeared, and partial response was defined as ≥30% reduction in the maximum cross-sectional diameter. Although it was difficult to distinguish the residual tumor tissue from radiation fibrosis, the observed residual density was considered free of local progression unless its size subsequently increased.

The Kaplan-Meier method was used to assess survival. Acute toxicities were assessed by the Common Toxicity Criteria (version 2.0), and late toxicities were scored according to the European Organization for Research and Treatment of Cancer/Radiation Therapy Oncology Group late radiation morbidity scoring scheme.

Table 1. Patient characteristics

Median age (range) (y)	75 (63–87)
Men/women (*n*)	30/7
Clinical stage* (IA/IB) (*n*)	17/20
Histology (SCC/adeno/others) (*n*)	15/15/7
Medically inoperable/refusal of surgery (*n*)	23/14
Total dose (70/80/88/94 Gy_E) (*n*)	3/17/16/1

Abbreviations: SCC = squamous cell carcinoma; adeno = adenocarcinoma.

* TNM classification.

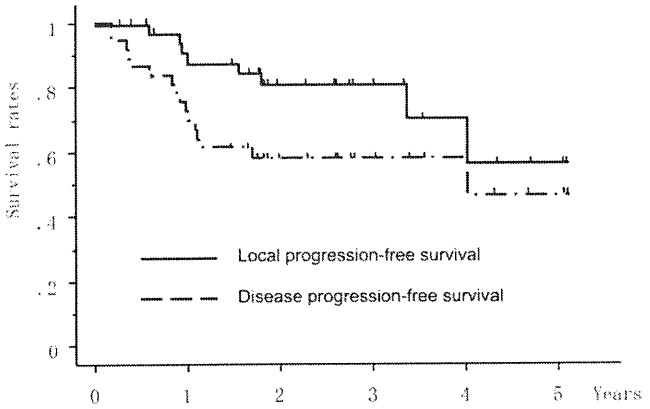

Fig. 1. Local progression-free and disease progression-free survival rates in all patients.

RESULTS

Between December 1999 and October 2003, 37 patients with Stage I NSCLC, including 10 patients enrolled in the dose escalation study, were treated by PBT in our institution. Patient characteristics are shown in Table 1.

The median duration of follow-up in all patients was 24 months (range, 3–62 months). The overall response rate was 86% (95% confidence interval [CI], 71–96%), but primary tumor regrowth occurred in 2 patients, at 7 and 12 months after treatment, respectively. The 1- and 2-year local progression-free survival rates, defined as no evidence of both primary tumor regrowth and death from any cause, were 91% (95% CI, 81–100%) and 80% (95% CI, 66–95%), respectively (Fig. 1). The corresponding disease progression-free survival rates were 73% (95% CI, 58–87%) and 58% (95% CI, 42–75%), respectively (Fig. 1). The overall survival rate at 2 years was 84% (95% CI, 71–97%) (Fig. 2).

Acute and late toxicities in all patients are shown in Table 2. Acute Grade 1 esophagitis was observed in 1 patient with T2 tumor (Stage IB) near the aortic arch who received a total dose of 88 Gy_E. Acute Grade 1 fever was observed in 1 patient with Stage IB disease who received a total dose of 80 Gy_E. No Grade 2 or greater acute toxicity was observed.

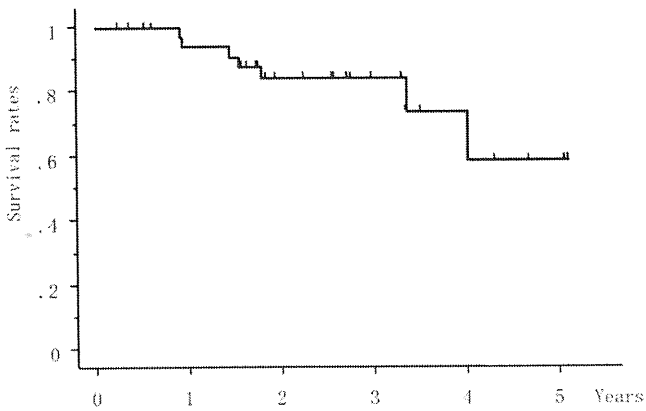

Fig. 2. Overall survival in all patients

Table 2. Acute and late toxicities

Toxicity	Grade	No. of patients
Acute		
Dermatitis	1	29
Esophagitis	1	1
Fever	1	1
Late		
Chest pain	1	4
Pulmonary*	1	25
	2	3
	3	3

* Including radiation pneumonitis and pleural effusion.

Late Grade 1 chest pain, consistent with the proton therapy field, was observed in 4 patients who received 80 or 88 Gy_E. Grade 2 and Grade 3 late pulmonary toxicities were observed in 3 patients each. They received 88 Gy_E of PBT, except for 1 patient who received 94 Gy_E. All Grade 2 pulmonary toxicities were radiation pneumonitis, which occurred from 4.5 to 8 months after the treatment. Two of the late Grade 3 pulmonary toxicities were pleural effusion requiring repeated drainage. One was observed at 9 months and the other at 23 months after treatment, with no evidence of disease progression. The other late Grade 3 pulmonary toxicity was radiation pneumonitis, treated by steroid pulse therapy and oxygen inhalation. It occurred 2.5 months after the beginning of PBT.

Late toxicities by clinical substage are shown in Table 3. Of 6 patients who suffered Grade 2 or greater late pulmonary toxicity, 5 had Stage IB disease.

The patterns of failure by clinical substage are shown in Table 4. Two local tumor regrowths were observed in Stage IB disease. Of the 5 patients who experienced pulmonary hilar or mediastinal lymph node recurrence without primary tumor regrowth, 4 had Stage IB disease. Distant relapse alone occurred equally in Stage IA and Stage IB. The locoregional relapse-free and overall survival curves in Stage IA and Stage IB are shown in Figs. 3 and 4. The 2-year locoregional relapse-free survival rates were 94% (95% CI, 58–100%) in Stage IA and 62% (95% CI, 38–81%) in Stage IB, and the 2-year overall survival rates were 83% (95% CI, 62–100%) in Stage IA and 82% (95% CI, 64–100%) in Stage IB.

Table 3. Late toxicities by clinical stage

Toxicity	All (n = 37)	Stage IA (n = 17)	Stage IB (n = 20)
Chest pain			
Grade 1	4	2	2
Pulmonary			
Grade 1	25	14	11
Grade 2	3	1	2
Grade 3	3	0	3

Table 4. Patterns of failure by clinical stage

Site	All (n = 37)	Stage IA (n = 17)	Stage IB (n = 20)
Local only	1	0	1
Locoregional	1	0	1
Regional only	5	1	4
Regional and distant	1	0	1
Distant only	6	3	3

DISCUSSION

Our results show that PBT is a promising treatment modality for Stage I NSCLC. Although the number of patients was small and the duration of follow-up was short, the 2-year local progression-free and overall survival rates were 80% (95% CI, 66–95%) and 82% (95% CI, 68–97%), respectively. Loma Linda University and Tsukuba University also reported similarly good results of PBT for Stage I NSCLC (11–13). At Loma Linda University, 68 patients were treated by a total dose of 51 Gy_E or 60 Gy_E in 10 fractions, and the 3-year disease-specific survival rate was 72% (12). At Tsukuba University, in 28 Stage I patients (Stage IA/IB, 9/19), the 2-year and 5-year cause-specific survival rates were 66% and 40%, respectively (13).

These results of PBT series are superior to those of conventional radiotherapy, for which 5-year overall survival rates range from only 5% to 30% (3–6). Stereotactic radiotherapy with photon beams, however, has been used to treat Stage I NSCLC in many institutions and produces better outcomes than conventional radiotherapy (14–17). Onishi *et al.* retrospectively reported the results of a Japanese multi-institutional study. The 3- and 5-year cause-specific survival rates were both 78% (17).

Stratifying the results of PBT series by clinical substage, the Loma Linda study showed increased tumor relapse rates in Stage IB patients compared with Stage IA patients (51% vs. 13% at 3 years), and overall survival in Stage IA patients was better than that in Stage IB patients (median survival, 39 months vs. 19 months) (12). Tsukuba University also

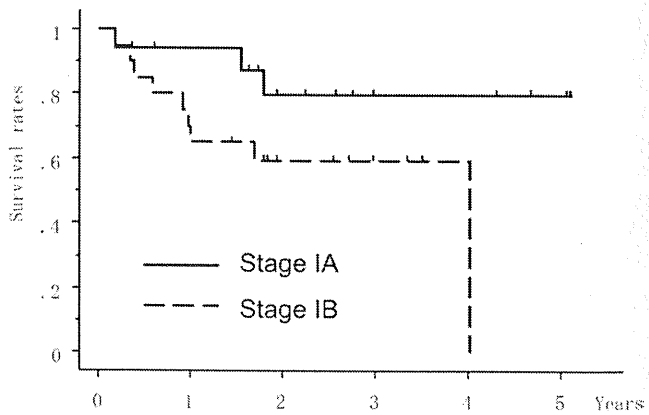

Fig. 3. Locoregional relapse-free survival rates in Stage IA and Stage IB disease.

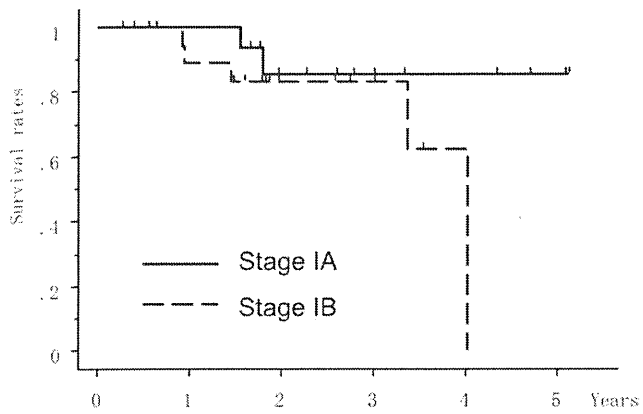

Fig. 4. Overall survival rates in Stage IA and Stage IB disease.

reported that Stage IA patients fared significantly better than did Stage IB patients both in 5-year cause-specific (88% vs. 23%) and disease-free survival rates (89% vs. 17%) (13). Similarly, in the present study, a poorer outcome was observed in Stage IB patients compared with Stage IA patients. Two patients who experienced local tumor regrowth both had Stage IB disease, and locoregional recurrences were observed more frequently in Stage IB disease (30% [95% CI, 12–54%]) than in Stage IA disease (6% [95% CI, 0–28%]) (Table 4, Fig. 3).

Thus, in Stage IA disease, the results of high-dose PBT alone might be comparable to those of surgical series. In Stage IB disease, however, the outcome remains poor. As discussed in the Tsukuba study (13), these results of PBT series in Stage IB patients suggest that clinical Stage IB patients might have had pathologically more advanced disease. The addition of elective nodal irradiation or systemic treatment could eradicate the microscopic nodal or distant diseases. Some randomized trials have recently suggested the significant benefit of adjuvant systemic therapy after surgical resection over surgery alone, even for pathologically proven Stage IB disease (18–20).

Another hypothesis explaining the poor outcomes in Stage IB disease was that the total doses used by the PBT series might be insufficient to control primary tumors. Larger tumors contain more malignant cells and more hypoxic areas, thus requiring higher radiation doses to be controlled. If the malignant disease is confined to the primary site, higher doses focusing on the primary tumor might prevent the malignant cells from metastasizing, thereby improving the outcomes in Stage IB diseases.

The acute toxicities of PBT were acceptable in the current study, as other institutions reported. As for late toxicities, the Loma Linda study reported no radiation pneumonitis requiring steroids or anti-inflammatory therapy (12). At Tsukuba University, among 51 patients with more advanced diseases, there were three Grade 2 and one Grade 3 lung toxicities approximately 3 months or longer after radiotherapy completion (13). In contrast, we experienced substantial late pulmonary toxicities. Six patients, corresponding to 16% (95% CI, 6–32%), suffered Grade 2 or greater late pulmonary toxicities.

One possible reason for the late pulmonary toxicities observed in the present study was that the total doses used in our institution were biologically higher than those used in other institutions. According to the linear–quadratic model, the biologic equivalent dose (BED) is defined as $D(1 + d/\alpha/\beta)$, in which D is the total dose, d is the daily dose, and α/β is assumed to be 10 for tumors. The BEDs for 70/80/88/94 Gy_E used in the current study were 95/112/127/138 Gy_{10}, whereas the BED used in the Loma Linda study was 96 Gy_{10} and those in the Tsukuba study were 90 Gy_{10} for Stage IA and 105 Gy_{10} for Stage IB. Six patients who experienced Grade 2 or greater late pulmonary toxicities in the present study received 88 Gy_E (127 Gy_{10}) or 94 Gy_E (138 Gy_{10}).

Independent of total dose, there are some considerations to explain pulmonary toxicities after PBT. The proton beam should stop at the distal margin of the target volume, but because aerated lung tissue is less dense than other soft tissues of the body, the proton beam might pass through beyond the target volume, and an unexpected high dose area might be generated in the surrounding normal lung. From a biologic viewpoint, because it is suggested that the relative biologic effectiveness of proton beams becomes larger at the distal end of their track, higher biologic lung dose behind the target volume potentially might be associated with the late pulmonary toxicities.

Another consideration is the tumor shrinkage during the treatment period. If overall treatment time is long enough for the tumor to respond to PBT and start shrinking, an aerated space appears where the tumor existed, and the proton beam will deliver excessive doses to the normal lung tissue both around and behind the reduced tumor in the target volume. A hypofractionation approach with a shorter treatment period can avoid this phenomenon. Proton beam therapy in the hypofractionation schedule can be finished before the tumor begins to shrink, and the planned dose should be completely delivered to the target volume. A hypofractionation strategy might be potentially more effective for the tumor and less toxic for the surrounding normal lung. Our PBT schedule required 4 to 5 weeks to complete the treatment, but a shorter overall treatment time with hypofractionation can be considered as a future strategy. Loma Linda University has been using a 2-week/10-fraction schedule, and some Japanese stereotactic radiotherapy institutions have already experienced shorter treatment schedules, within 1 week (12, 14, 15).

Another concern with late pulmonary toxicities is the target volume. Of 6 patients who developed Grade 2 or greater pulmonary toxicities, 5 had Stage IB disease. As the target volume increases, naturally the volume of the irradiated normal lung becomes larger, and the risk of pulmonary toxicities gets higher.

From these findings and discussions, the PBT schedule for Stage IB patients should be reconsidered. As discussed above, if the malignant cells are confined to the primary tumor, higher doses to the primary tumor can lead to better

local tumor control and reduce both locoregional and distant relapse in Stage IB diseases; but in contrast, it also includes more risk of generating pulmonary toxicities. Therefore, although there might be an opportunity for further dose escalation for Stage IB disease, it should be cautiously examined only on a prospective clinical study basis.

In Stage IA patients, the results of high-dose PBT alone might be comparable to those of surgical series. To further enhance its efficacy and reduce its toxicity, a hypofractionation schedule is considered to be a promising future strategy. More data from prospective clinical trials will be needed to confirm the benefit of PBT in the future.

REFERENCES

1. Ginsgerg RJ, Rubinstein LV. Randomized trial of lobectomy versus limited resection for T1 N0 non-small cell lung cancer. Lung Cancer Study Group. *Ann Thorac Surg* 1995;60:615–622.
2. Adebonojo SA, Bowser AN, Moritz DM, *et al.* Impact of revised stage classification of lung cancer on survival: a military experience. *Chest* 1999;115:1507–1513.
3. Harpole DH Jr., Herndon JE Jr., Young WG, *et al.* Stage I nonsmall cell lung carcinoma. A multivariate analysis of treatment methods and patterns of recurrence. *Cancer* 1995;76:787–796.
4. Martini N, Bains MS, Burt ME, *et al.* Incidence of local recurrence and second primary tumors in resected stage I lung cancer. *J Thorac Cardiovasc Surg* 1995;109:120–129.
5. Graham PH, Gebski VJ, Langlands AO. Radical radiotherapy for early non–small-cell lung cancer. *Int J Radiat Oncol Biol Phys* 1995;31:261–266.
6. Mehta M, Scrimger R, Mackie R, *et al.* A new approach to dose escalation in non–small-cell lung cancer. *Int J Radiat Oncol Biol Phys* 2001;49:23–33.
7. Zimmermann FB, Bamberg M, Molls M, *et al.* Radiation therapy alone in early stage non-small cell lung cancer. *Semin Surg Oncol* 2003;21:91–97.
8. Ogino T, Murayama S, Itou Y, *et al.* Three-dimensional positioning verification by image subtraction method using real-time digital radiography [Abstract]. *Int J Radiat Oncol Biol Phys* 2000;48(Suppl. 1):195.
9. Ando K, Furusawa Y, Suzuki M, *et al.* Relative biological effectiveness of the 235 MeV proton beams at the National Cancer Center Hospital East. *J Radiat Res* 2001;42:79–89.
10. Therasse P, Arbuck SG, Eisenhauer EA, *et al.* New guidelines to evaluate the response to treatment in solid tumors. *J Natl Cancer Inst* 2000;92:205–216.
11. Bush DA, Slater JD, Bonnet R, *et al.* Proton-beam radiotherapy for early-stage lung cancer. *Chest* 1999;116:1313–1319.
12. Bush DA, Slater JD, Shin BB, *et al.* Hypofractionated proton beam radiotherapy for stage I lung cancer. *Chest* 2004;126:1198–1203.
13. Shioyama Y, Tokuuye K, Okumura T, *et al.* Clinical evaluation of proton radiotherapy for non–small-cell lung cancer. *Int J Radiat Oncol Biol Phys* 2003;56:7–13.
14. Uematsu M, Shioda A, Suda A, *et al.* Computed tomography-guided frameless stereotactic radiotherapy for Stage I non–small-cell lung cancer: A 5-year experience. *Int J Radiat Oncol Biol Phys* 2001;51:666–670.
15. Nagata Y, Negoro Y, Aoki T, *et al.* Clinical outcomes of 3D conformal hypofractionated single high-dose radiotherapy for one or two lung tumors using a stereotactic body frame. *Int J Radiat Oncol Biol Phys* 2002;52:1041–1046.
16. Timmerman R, Papiez L, McGarry R, *et al.* Extracranial stereotactic radioablation. Results of a phase I study in medically inoperable stage I non-small cell lung cancer. *Chest* 2003;124:1946–1955.
17. Onishi H, Araki T, Shirato H, *et al.* Stereotactic hypofractionated high-dose irradiation for stage I nonsmall cell lung carcinoma. Clinical outcomes in 245 subjects in a Japanese mutiinstitutional study. *Cancer* 2004;101:1623–1631.
18. Winton TL, Livingston R, Johnson D, *et al.* National Cancer Institute of Canada Clinical Trials Group, National Cancer Institute of the United States Intergroup JBR. 10 Trial Investigators. Vinorelbine plus cisplatin vs. observation in resected non-small cell lung cancer. *N Engl J Med* 2005;352:2589–2597.
19. Strauss GM, Herndon J, Maddaus MA, *et al.* Randomized clinical trial of adjuvant chemotherapy with paclitaxel and carboplatin following resection in stage IB non-small cell lung cancer (NSCLC): Report of Cancer and Leukemia Group B (CALGB) Protocol 9633 [Abstract]. *Proc Am Soc Clin Oncol* 2004;7019.
20. Kato H, Ichinose Y, Ohta M, *et al.* A randomized trial of adjuvant chemotherapy with uracil-tegafur for adenocarcinoma of the lung. *N Eng J Med* 2004;350:1713–1721.

Int J Clin Oncol (2007) 12:3–7
DOI 10.1007/s10147-006-0646-6

© The Japan Society of Clinical Oncology 2007

REVIEW ARTICLE

**Yasushi Nagata · Yukinori Matsuo · Kenji Takayama
Yoshiki Norihisa · Takashi Mizowaki
Michihide Mitsumori · Keiko Shibuya · Shinsuke Yano
Yuichiroh Narita · Masahiro Hiraoka**

Current status of stereotactic body radiotherapy for lung cancer

Received: December 5, 2006

Abstract Stereotactic radiotherapy (SRT) for extracranial tumors has been recently performed to treat lung and liver cancers, and has subsequently been named stereotactic body radiotherapy (SBRT). The advantages of hypofractionated radiotherapy for treating lung tumors are a shortened treatment course that requires fewer trips to the clinic than a conventional program, and the adoption of a smaller irradiated volume allowed by greater setup precision. This treatment is possible because the lung and liver are considered parallel organs at risk. The preliminary clinical results, mostly reported on lung cancer, have been very promising, including a local control rate of more than 90%, and a relatively low complication rate. The final results of a few clinical trials are awaited. SBRT may be useful for the treatment of stage I lung tumors.

Key words Stereotactic body radiotherapy · Conformal radiotherapy · Lung cancer · Stereotactic body frame · Stereotactic radiotherapy · Extracranial tumors

Introduction

Stereotactic radiotherapy (SRT) for extracranial tumors has been recently performed to treat extracranial tumors, mainly lung and liver cancers, and has subsequently been named stereotactic body radiotherapy (SBRT) or extracranial stereotactic radiotherapy (ESRT). The advantages of hypofractionated radiotherapy for treating lung tumors are a shortened treatment course that requires fewer trips to the clinic than a conventional program, and the adoption of a smaller irradiated volume allowed by greater setup precision. This treatment is possible because the lung and liver are considered parallel organs at risk (OAR). The disadvantages of SBRT are the uncertain effects of altered fractionation and the theoretical risk of worsening the ratio of normal tissue to tumor tissue through the use of a high dose per fraction. In this article, the technical procedures and clinical results of SBRT, especially in lung cancer, are reviewed.

Y. Nagata (✉) · Y. Matsuo · K. Takayama · Y. Norihisa · T. Mizowaki · M. Mitsumori · K. Shibuya · S. Yano · Y. Narita · M. Hiraoka
Department of Therapeutic Radiology and Oncology, Kyoto University, Graduate School of Medicine, Sakyo, Kyoto 606-8507, Japan
Tel. +81-75-751-3762; Fax +81-75-751-3418
e-mail: nag@kuhp.kyoto-u.ac.jp

Biology

The biological background of SBRT is important. There is no past clinical evidence for this kind of hypofractionated regimen to extracranial tumors; therefore, most clinical regimens should be based on biological estimations.

The two great issues in hypofractionated regimens are dose response for tumor control and toxicity to normal tissue. Can the conventional linear-quadratic (LQ) model be applied in the SBRT dose range? Can repopulation be avoided in the SBRT regimen? How great is the effect of hypoxia in SBRT?

Fowler et al.[1] answered these questions, which are mostly applicable to SBRT; however, they recommended that SBRT be performed three to five fractionated schedule rather than using single SRS. These biological speculations should be reconfirmed in the clinical setting.

Body fixation

The first body fixation device was introduced in clinical practice as a stereotactic body frame by Bromgren et al.[2] and Lax et al.[3] Patients were fixed in the stereotactic frame, using a vacuum pillow. The concept of this frame is to utilize the cranial SRT coordinates for extracranial SBRT. The difference between cranial SRT and extracranial SBRT is the accuracy of the setup. The Japanese national guidelines for SRT state that the allowance of setup error is 2 mm for cranial tumors and 5 mm for extracranial tumors.

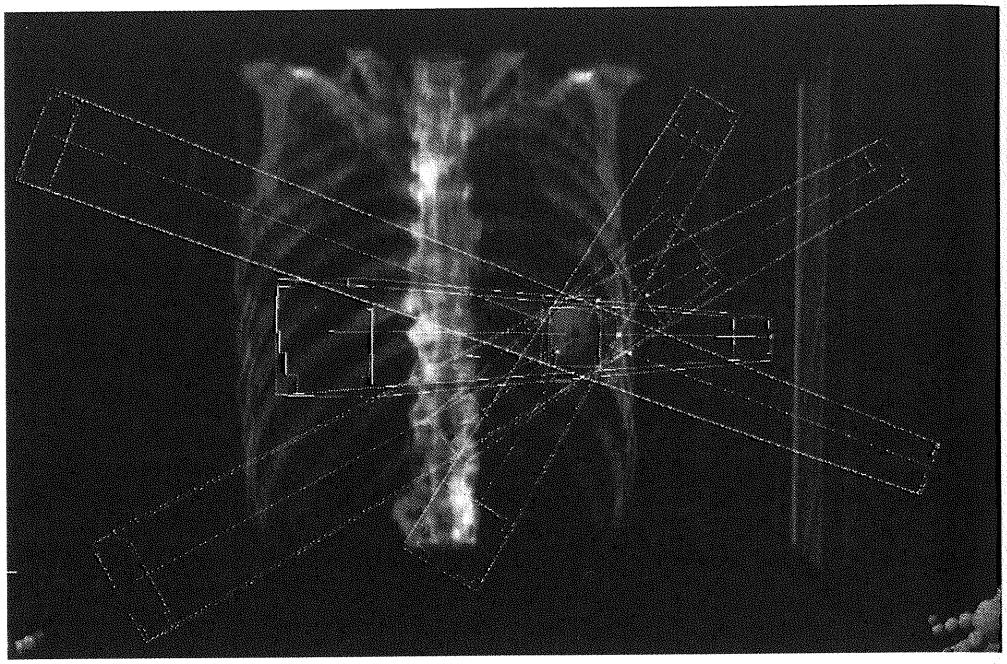

Fig. 1. Stereotactic body radiotherapy (SBRT) for lung cancer. In this image for treatment planning for left lung cancer, five beams are focused on the target

Some other fixing apparatuses using a vacuum sheet or thermoplastic shell are clinically available.

Respiratory monitoring

In the clinical practice of SBRT, the regulation of respiratory movement is essential. There are three ways to regulate the respiration of patients: respiratory holding, respiratory regulation, and respiratory gating.

The respiratory holding method is to ask patients to hold their breath for about 10 s during radiation; therefore, radiation is performed intermittently four to ten times. Theoretically, this method can reduce the internal target volume (ITV). Holding can be done either voluntarily by patients or by using devices such as an active breathing control (ABC).

Respiratory regulation can be performed by exerting pressure on the abdomen using a plate like our diaphragm control or an abdominal belt.[4]

The respiratory gating method was originally developed in Japan. The gating sensors are a respiratory flow monitor, abdominal wall fiducials, and implanted gold fiducials.

Target definition

In computed tomography (CT) images taken under free-breathing long-scan (4–8 s) conditions, the target outlines of the ITV are delineated. These CT images include the respiratory movement of the target. ITVs and Clinical Target Volume (CTV)s were not edited for anatomy.

If patients are irradiated with gated radiotherapy, the target outlines of CTV could be delineated under gating conditions.

The setup margins between the ITV and the planning target volume (PTV) must be determined at each institution. Our margins are 5 mm for the anteroposterior (AP), 5 mm for the lateral, and 8–10 mm for the craniocaudal directions. Overlapping the outlines under inhale and exhale conditions is an alternative choice.

Treatment planning

There are two different concepts of Radiotherapy Treatment Planning (RTP) for SBRT. One concept, mainly used in Japan, is to maintain dose homogeneity within the target. In this case, the dose is usually prescribed at the isocenter. The other concept, mainly used in the United States, is not to maintain dose homogeneity. In this case, the dose is prescribed at the PTV margin. Our method adheres to the former concept, with selection of the optimal direction of noncoplanar beams, with the goal of the RTP being 6–10 portals for noncoplanar static beams, as shown in Fig. 1. The beam energy used was 6 MV and the isocenter was single for all beams. Four single treatments with 12 Gy of radiation were prescribed at the isocenter. Using an LQ model,[5] the Biological Effective Dose (BED) was here defined to be nd (1 + d / alpha-beta) Gy, where n is the fractionation number, d is the daily dose, and the alpha-beta ratio for tumors was assumed to be 10. The value was 105.6 Gy-BED for 48 Gy in four fractions. The most important issue for RTP in SBRT is to maintain the dose constraints of OAR to avoid serious complications. The dose constraints of the OAR, including the spinal cord, pulmonary artery, bronchus, and heart, under the Japan Clinical Oncology Group (JCOG) 0403 protocol, are shown in Table 1.

Verification before radiation

In the clinical practice of SBRT for lung cancer, verification before each treatment is mandatory. In our institute, before each treatment, AP and lateral portal films are taken for verification. The position of each patient is verified by three experienced oncologists and technologists for each treatment. When the setup errors are larger than 2 mm between the X-ray simulation film and portal film in any direction, the patient is repositioned and portal films are taken and verified again. CT on rails and FOCAL units are also useful materials for verification before each treatment.

Clinical indications for SBRT

Currently, the eligibility criteria for patients with primary lung cancer are: (1) tumor size less than 5 cm in diameter without nodal and distant metastases (T14N0M0); (2) surgery was contraindicated or refused; (3) the patient could remain stable in the body frame for longer than 30 min (WHO performance status <=2); (4) no active interstitial pneumonitis; and (5) written informed consent was obtained. The criteria for patients with secondary lung cancer are: (1) tumor size less than 5 cm in diameter; (2) tumor number three or less; (3) no other metastases, and (4) local tumor is controlled.

Tumor size is an important factor when dose homogeneity within the target should be maintained. The dose constraints of mediastinal organs should be maintained; therefore, a central tumor could be less suitable for SBRT indications than a peripheral tumor.

Table 1. Dose constraints of various organs at risk, according to the JCOG 0403 protocol

Organ	Dose	Volume	Dose	Volume
Lung	40 Gy	<=100 cc	MLD	<=18 cc
	V15	<=25%	V20	<=20%
Spinal cord	25 Gy	Max		
Esophagus	40 Gy	<=1 cc	35 Gy	<=10 cc
Pulmonary artery	40 Gy	<=1 cc	35 Gy	<=10 cc
Stomach	36 Gy	<=10 cc	30 Gy	<=100 cc
Intestine	36 Gy	<=10 cc	30 Gy	<=100 cc
Trachea, main bronchus	40 Gy	<=10 cc		
Other organs (heart, etc)	48 Gy	<=1 cc	40 Gy	<=10 cc

18-Fluoro-deoxy-glucose (FDG)-positron emission tomography (PET)

18-Fluoro-deoxy-glucose (FDG)-PET scanning is an important examination both for the staging and the follow-up of lung cancer. For lung cancer staging, occult mediastinal and hilar lymph nodes, and distant metastases, are frequently found by FDG-PET.

In the follow-up of lung cancer after SBRT, radiation fibrotic change cannot be distinguished from residual tumor. FDG-PET is also useful in this situation.[6]

Clinical results

Local tumor response

The local control rates of primary lung cancer with SBRT have been previously reported by several authors, as shown in Table 2: 94 % (47/50) for 50–60 Gy in five fractions with a median follow-up of 36 months,[7] 92 % (22/24) for 60 Gy in 8 fractions with a median follow-up of 24 months,[8] 81% (30/37) for 60 Gy in three fractions with a median follow-up of 15 months,[9] 80% for 48–60 Gy in eight fractions with a median follow-up of 17 months,[10] 95% for 45–56.2 Gy in three fractions with a median follow-up of 10 months,[11] 90% for 30–40 Gy in four fractions with a median follow-up of 21 months,[12] and 98% (44/45) for 48 Gy in four fractions with a median follow-up of 30 months.[13] However, the definition of local control after radiotherapy is difficult because local tumor failure and Radiation Induced Lung Damage (RILD) cannot be clearly delineated. Even though the definition of local control is different in various trials, a BED larger than 100 Gy may be effective for the SRT of solitary lung cancer with a local control rate of above 85%.

Survival

The survival rates of stage IA (T1N0M0) lung cancer and stage IB (T2N0M0) lung cancer have not been separately reported by several authors. In our stage IA series, the 1-year and 5-year local relapse-free survival rates were 100% and 95%. The isease-free survival rates after 1, 3, and 5 years were 80%, 72%, and 72%, respectively, and the overall survival rates were 93%, 83%, and 83%, respectively. In our stage IB series, the 1-year local relapse-free survival

Table 2. Local control rates of stereotactic radiotherapy for primary lung cancer

Author (year)	Total dose (Gy)	Daily dose (Gy)	Reference point	Local control	Median follow-up (months)
Uematsu[7] (2001)	50–60	10	80% Margin	94% (47/50)	36
Arimoto[8] (1998)	60	7.5	Isocenter	92% (22/24)	24
Timmerman[9] (2003)	60	20	80% Margin	81% (30/37)	15
Onimaru[10] (2003)	48–60	6–7.5	Isocenter	80% (20/25)	17
Wulf[11] (2004)	45–56.2	15–15.4	80% Margin	95% (19/20)	10
Nagata[13] (2005)	48	12	Isocenter	98% (44/45)	30
Lee[12] (2003)	30–40	10	90% Margin	90% (8/9)	21

Table 3. Clinical toxicities after stereotactic radiotherapy for primary lung cancer

Author (year)	Number of cases	Lung >=grade 3	Lung grade 5	Other grade 5
Uematsu[7] (2001)	50	0%	0	
Arimoto[8] (1998)	24	NA	0	
Lee[12] (2003)	28	0	0%	
Onimaru[10] (2003)	45	2%	0%	Esophagus
Wulf[11] (2004)	61	0	0%	
Nagata[13] (2005)	45	0	0	
Timmerman[16] (2006)	70	20%	9%	Hemoptysis, pericarditis
J-CERG[5] (2006)	2106	NA	0.50%	Esophagus, hemoptysis

NA, not available

rate was 100%. The disease-free survivals after 1, 3, and 5-years were 92%, 71%, and 71%, respectively, and the overall survival rates were 82%, 72%, and 72%, respectively.[13] Onishi et al.[14] recently reported the results for 13 institutions in Japan, which summarized findings for 245 patients: 155 with stage IA lung cancer and 90 with stage IB lung cancer. There were 87 operable and 158 inoperable patients, and their results showed that the intercurrent death rate was especially high in the inoperable patient group. Moreover, the 5-year survival rates of operable patients irradiated with more than BED=100 Gy was 90% for stage IA and 84% for stage IB, and their clinical results were as good as those for surgery.

These survival rates should be compared with the results of surgery; however, the results of SBRT may differ depending on how many of the group are operable and how many are inoperable, and how many of the tumors are central and how many, peripheral.

Toxicities

The great concern of pulmonary toxicity with this SBRT treatment was relieved by the very low rates of complications in early studies. Most pulmonary complications were less than National Cancer Institute common toxicity criteria (NCI-CTC) version 2.0 grade 2. No other serious complications were reported, except for rib fracture, intercostals neuralgia, and mild dermatitis. However, recently, a few serious complications have been reported by several institutions in Japan.[15] These complications include grade 5 pulmonary complications, radiation pneumonitis, hemoptysis, and radiation esophagitis. Most cases of grade 5 radiation pneumonitis were associated with interstitial pneumonitis. Cases of interstitial pneumonitis should be carefully considered. Thoraco-cutaneous fistula was reported in a patient with previous tuberculosis history. Acute cholecystitis was reported in a patient with gallstones who had been pressed with an abdominal press board at the time of SBRT.

Another toxicity concern was the effect on the central bronchus, pulmonary artery, esophagus, heart, and spinal cord. The effects of a hypofractionated dose on the main bronchus, pulmonary artery, heart, and esophagus have not been followed up for a sufficiently long time. Lethal pulmonary bleeding and esophageal ulcer have been reported previously by several authors. Timmerman et al.[16] recently reported a series of complications with SBRT. Central hilar tumors adjacent to mediastinal organs should be carefully considered.[17] Table 3 shows the toxicities reported by various groups.

Ongoing clinical trials

Recently, a multi-institutional phase II study of SBRT for T1N0M0 non-small cell lung cancer under JCOG (http://www.jcog.jp/) protocol 0403 was started in Japan. Sixteen institutions entered together and started the same 48-Gy SBRT dose at the isocenter in four fractions for T1N0M0 lung cancer. One hundred patients have been registered. The results of SBRT for both inoperable and operable stage I lung cancer patients are awaited.

A new dose-escalation study of SBRT for T2N0M0 lung cancer is also planned, under the JCOG.

Timmerman et al.[9] concluded that a 60-Gy marginal dose in three fractions was the limiting dose, and the Radiation Therapy Oncology Group (RTOG) study 0239 for inoperable patients is already closed. There are a few other reports so far.[18-23] The coming RTOG protocols for operable patients, central tumors, and lung metastases are awaited.

Future directions

Both a new IGRT technique and four-dimensional RTP are future directions of SBRT. Systemic chemotherapy may be considered when the local tumor is well controlled and regional/distant metastases are frequent.

The primary indication for stereotactic radiotherapy in lung cancer could be a stage 1A (T1N0M0) patient. Very early-stage lung cancer can now be detected by screening CT examination, and these cases are also good indications for SRT; however, the issue in these cases is histological confirmation. In our clinical experience, 7 of a total of 95 SRT cases could not be finally confirmed histologically. Of course, these 7 cases were not included in our study.[13] They could not be histologically confirmed because of failure or difficulty in CT-guided biopsy or transbronchoscopic lung biopsy (TBLB). Currently, CT screening has revealed very early-stage lung cancer with ground glass opacity (GGO) and some patients with severe emphysema could be contraindicated for biopsy. Therefore, the indication for SRT for

these cases without histological confirmation should be discussed in the future. When the tumor is larger than 3 cm in diameter, which corresponds to stage 1B (T2N0M0), SRT is possible; however, the intratumor dose becomes less homogeneous, and the rate of occult distant metastases may increase. Therefore, extension of the indication of this technique for T2 tumors requires more consideration for dose escalation or adjuvant chemotherapy.

The current standard choice for stage IA lung cancer treatment is lobectomy;[24] however, for many patients this is not indicated because of accompanying diseases, such as chronic obstructive pulmonary disease (COPD), cardiac disease, and diabetes. For such patients, various minimal surgical techniques are indicated, including wedge resection and video-assisted thoracoscopic surgery (VATS), as well as ablation. The local control rates of various other modalities for primary stage I lung cancer previously reported were 93% for wedge resection and 83%-95% for VATS, and the 5-year survival rates were 82% and 50%-70%, respectively. A further randomized trial comparing SBRT with surgery should be considered.

Conclusion

SBRT is a safe and effective treatment method for stage I lung tumors. Further clinical studies are therefore warranted.

Acknowledgments This work was supported by Grant-in-aid No. 18390333, of the Ministry of Education and Science, Japan, and Grant-in-aid No. H18-014, of the Ministry of Health, Welfare, and Labor, Japan. The authors gratefully acknowledge Mr. Daniel Mrozek for his editorial assistance.

References

1. Fowler JF, Tome WA, Fenwick JD, Mehta MP (2004) A challenge to traditional radiation oncology. Int J Radiat Oncol Biol Phys 60:1241–1256
2. Blomgren H, Lax I, Goeranson H, et al. (1998) Radiosurgery for tumors in the body: clinical experience using a new method. J Radiosurg 1:63–74
3. Lax I, Blomgren H, Larson D, et al. (1998) Extracranial stereotactic radiosurgery of localized target. J Radiosurg 1:135–148
4. Negoro Y, Nagata Y, Aoki T, et al. (2001) The effectiveness of an immobilization device in conformal radiotherapy for lung tumor: reduction of respiratory tumor movement and evaluation of daily set-up accuracy. Int J Radiat Oncol Biol Phys 50:889–898
5. Yaes RJ, Patel P, Maruyama Y (1991) On using the linear-quadratic model in daily clinical practice. Int J Radiat Oncol Biol Phys 20:1353–1362
6. Ishimori T, Saga T, Nagata Y, et al. (2004) 18F-FDG and 11C-Methionine evaluation of the treatment response of lung cancer after stereotactic radiotherapy. Ann Nuclear Med 18:669–674
7. Uematsu M, Shioda A, Tahara K, et al. (2001) Computed tomography-guided frameless stereotactic radiotherapy for stage I non-small-cell lung cancer: a 5-year experience. Int J Radiat Oncol Biol Phys 51:666–670
8. Arimoto T, Usubuchi H, Matsuzawa T, et al. (1998) Small volume multiple non-coplanar arc radiotherapy for tumors of the lung, head & neck and the abdominopelvic region. In: Lemke HU (ed) CAR'98 Computer assisted radiology and surgery. Elsevier, Tokyo
9. Timmerman R, Papiez L, McGarry R et al. (2003) Extracranial stereotactic radioablation: results of a phase I study in medically inoperable stage I non-small cell lung cancer. Chest 124:1946–1955
10. Onimaru R, Shirato H, Shimizu S, et al. (2003) Tolerance of organs at risk in small-volume, hypofractionated, image-guided radiotherapy for primary and metastatic lung cancers. Int J Radiat Oncol Biol Phys 56:126–135
11. Wulf J, Haedinger U, Oppitz U, et al. (2004) Stereotactic radiotherapy for primary lung cancer and pulmonary metastases: a non-invasive treatment approach in medically inoperable patients. Int J Radiat Oncol Biol Phys 60:186–196
12. Lee S, Choi EK, Park HJ, et al. (2003) Stereotactic body frame based fractionated radiosurgery in the consecutive days for primary and metastatic tumor in the lung. Lung Cancer 40:309–315
13. Nagata Y, Negoro Y, Aoki T, et al. (2005) Clinical outcomes of a phase I/II study of 48 Gy of stereotactic body radiation therapy in four fractions using a stereotactic body frame. Int J Radiat Oncol Biol Phys 63:1427–1431
14. Onishi H, Araki T, Shirato H, et al. (2004) Stereotactic hypofractionated high-dose irradiation for stage I non-small cell lung carcinoma. Cancer 101:1623–1631
15. Nagata Y, Matsuo Y, Takayama K, et al. (2006) Survey of SBRT in Japan. Int J Radiat Oncol Biol Phys 66(Suppl. 1):s150–151
16. Timmerman R, McGarry R, Yiannoutsos C, et al. (2006) Excessive toxicity when treating central tumors in a phase II study of stereotactic body radiation therapy for medically inoperable early-stage lung cancer. JCO 24:4833–4839
17. Joyner M, Salter BJ, Papanikolaou N, Fuss M (2006) Stereotactic body radiation therapy for centrally located lung lesions. Acta Oncol 45:802–807
18. Baumann P, Nyman J, Lax I, et al. (2006) Factors important for efficacy of stereotactic body radiation therapy of medically inoperable stage I lung cancer. A retrospective analysis of patients in the Nordic countries. Acta Oncol 45:787–795
19. Liu R, Buatti JM, Howes TL, et al. (2006) Optimal number of beams for stereotactic body radiotherapy of lung and liver tumors. Int J Radiat Oncol Biol Phys 66:906–912
20. Kimura T, Matsuura K, Murakami Y, et al. (2006) CT appearance of radiation injury of the lung and clinical symptoms after stereotactic body radiation therapy (SBRT) for lung cancers: are patients with pulmonary emphysema also candidates for SBRT for lung cancers? Int J Radiat Oncol Biol Phys 66:483–491
21. Herfarth KK, Debus J, Lohr F, et al. (2000) Stereotactic single dose radiation treatment of tumors in the lung. Radiology 217(Suppl.):148
22. McGarry RC, Papiez L, Williams M, et al. (2005) Stereotactic body radiation therapy of early-stage non-small-cell lung cancer: phase I study. Int J Radiat Oncol Biol Phys 63:1010–1015
23. Beitler JJ, Badine EA, El-Savah D, et al. (2006) Stereotactic body radiation therapy for nonmetastatic lung cancer. An analysis of 75 patients over 5 years. Int J Radiat Oncol Biol Phys 65:100–106
24. Lung Cancer Study Group (1995) Randomized trial of lobectomy versus limited resection for T1N0 non-small cell lung cancer. Ann Thorac Surg 60:615–623
25. Luketich JD, Ginsberg RJ (1996) Limited resection versus lobectomy for stage I non-small cell lung cancer. In: Pass HI, Mitchell JB, Johnson DH, et al. Lung cancer: Principles and Practice. Lippincott-Raven, Philladelphia, pp 561–566

改訂第2版

放射線治療マニュアル

編著

京都大学教授　平岡真寛

新潟大学教授　笹井啓資

大阪大学名誉教授　井上俊彦

中外医学社

執筆者（執筆順）

平岡　真寛　京都大学大学院医学研究科放射線腫瘍学・画像応用治療学教授
晴山　雅人　札幌医科大学大学院医学研究科放射線治療診断学教授
大内　　敦　札幌医科大学医学部放射線医学
舘岡　邦彦　札幌医科大学大学院医学研究科放射線治療診断学
西臺　武弘　京都医療技術短期大学教授
土器屋卓志　埼玉医科大学放射線腫瘍科教授
永田　　靖　京都大学大学院医学研究科放射線腫瘍学・画像応用治療学助教授
溝脇　尚志　京都大学大学院医学研究科放射線腫瘍学・画像応用治療学
白土　博樹　北海道大学医学部放射線部助教授
井上　武宏　大阪大学大学院医学系研究科放射線治療学教授
広川　　裕　医療法人社団葵会学術理事
小野　公二　京都大学原子炉実験所附属粒子線腫瘍学研究センターセンター長/教授
西村　恭昌　近畿大学医学部放射線腫瘍学教授
芝本　雄太　名古屋市立大学大学院医学研究科量子放射線医学教授
末山　博男　新潟県立中央病院放射線科診療部長
今田　　肇　産業医科大学放射線科助教授
寺嶋　廣美　九州大学保健学部教授
田中　良明　日本大学医学部放射線医学教授
今城　吉成　川崎医科大学放射線科教授
澁谷　　均　東京医科歯科大学医歯学総合研究科腫瘍放射線医学教授
茶谷　正史　大阪労災病院放射線科第２放射線科部長
手島　昭樹　大阪大学大学院医学系研究科医学物理工学教授
村山　重行　静岡がんセンター陽子線治療科部長
徳植　公一　筑波大学大学院人間総合科学研究科先端応用医学専攻助教授
早川　和重　北里大学医学部放射線科学教授

根本　建二　東北大学大学院医学系研究科放射線腫瘍学分野助教授
光森　通英　京都大学大学院医学研究科放射線腫瘍学・画像応用治療学講師
吉村　　均　高清会高井病院放射線科部長
玉本　哲郎　奈良県立医科大学放射線腫瘍医学講師
大原　　潔　筑波大学臨床医学系放射線腫瘍科助教授
唐澤　克之　都立駒込病院放射線科部長
清水わか子　君津中央病院放射線科医長
山下　　孝　癌研有明病院放射線治療科部長
小口　正彦　癌研有明病院放射線治療科副部長
秋元　哲夫　群馬大学大学院医学系研究科腫瘍放射線医学
三橋　紀夫　東京女子医科大学放射線医学教授
笹井　啓資　新潟大学大学院医歯学総合研究科腫瘍放射線医学教授
伊東　久夫　千葉大学大学院医学研究院放射線医学教授
宇野　　隆　千葉大学大学院医学研究院放射線医学助教授
磯部　公一　千葉大学医学部附属病院放射線科
兼平　千裕　東京慈恵会医科大学放射線医学講座教授
小泉　雅彦　京都府立医科大学放射線診断治療学講師
西山　謹司　大阪府立成人病センター放射線治療科部長
正木　英一　国立成育医療センター放射線診療部長
早渕　尚文　久留米大学医学部放射線科教授
中島　俊文　天理よろづ相談所病院放射線部治療部門部長
広田佐栄子　高槻病院放射線科
大屋　夏生　熊本大学医学薬学研究部放射線治療医学分野教授
井上　俊彦　大阪大学名誉教授

2 治療計画の手順

1 はじめに

放射線治療計画（以下，治療計画）は腫瘍に対し最適な線量を照射し，腫瘍周辺の正常組織に対する被曝を最小にするために放射線ビームの方向，形状および数などを決定する作業工程である．具体的には，患者の体位決定と固定，治療計画画像の収集，標的容積と決定臓器の抽出，照射法の決定，線量計算および線量分布検証をへてから照射が行われる[1]（**表 2-1**）．

実際には，放射線治療装置を模擬する X 線シミュレータや computed tomography（以下，CT）を用いた CT シミュレータなどを用いる．これらは，臨床的画像情報〔magnetic resonance（MR），positron emission tomography（PET）と ultrasound（US）などの解剖・生理学的（機能的）な画像情報など〕を参照した上で病巣部位に対して照射領域を設定することで行われる．

三次元治療計画装置はコンピュータ，機械工学や情報処理技術の進歩により発展を遂げ，現在では多くの施設で導入され，上記で示した臨床的画像情報を治療計画装置で利用が可能となっている[2,3]．同様に，直線加速器もより安定および高精度化となってきた．照射野の成型も単一 block から multi-leaf collimator（以下，MLC）を用いて行われるようになり，さらに，leaf 幅も 1 cm から 0.3 cm のものが利用可能となり，より腫瘍に限局させることが容易になってきた．

高精度放射線治療においてはビームの照射中に直線加速器の架台（ガントリ）を回転する運動照射，さらに各ガントリ回転角度における MLC の形状を腫瘍の形状に沿って動的に変更する原体回転照射が行われている．さらに，MLC などを用いた二次元における強度変調技術を可能にする強度変調放射線治療 intensity modulation radiation therapy（以下，IMRT）が開発され，腫瘍への一層の線量集中と腫瘍周辺の organ at risk（OAR）や正常組織の温存を図れるよう